LANGMUIR Article
Cite This: *Langmuir* 2018, 34, 15681−15688
pubs.acs.org/Langmuir

Reactive Molecular Dynamics Simulations of Thermal Film Growth from Di-*tert*-butyl Disulfide on an Fe(100) surface

Karen Mohammadtabar,[†] Stefan J. Eder,[‡,§] Pedro O. Bedolla,[‡] Nicole Dörr,[‡] and Ashlie Martini*[,†]

[†]Department of Mechanical Engineering, University of California Merced, 5200 N. Lake Road, Merced, California 95343, United States

[‡]AC2T research GmbH, Viktor-Kaplan-Straße 2/C, 2700 Wiener Neustadt, Austria

[§]Institute for Engineering Design and Logistics Engineering, Vienna University of Technology, Getreidemarkt 9, 1060 Vienna, Austria

ABSTRACT: Iron sulfide films are present in many applications, including lubricated interfaces where protective films are formed through the reactions of lubricant additive molecules with steel surfaces during operation. Such films are critical to the efficiency and useful lifetime of moving components. However, the mechanisms by which films form are still poorly understood because the reactions occur between two surfaces and so cannot be directly probed experimentally. To address this, we explore the thermal contribution to film formation of di-*tert*-butyl disulfide—an important extreme pressure additive—on an Fe(100) surface using reactive molecular dynamics simulations, where the reactive potential parameters are validated by comparison to ab initio calculations. The reaction pathway leading to the formation of iron sulfide surfaces is characterized using the reactive simulations. Then, the film formation process is mimicked by simulations where di-*tert*-butyl disulfide molecules are cyclically added to the surface and subjected to temperatures comparable to those expected due to frictional heating. The use of a reactive empirical potential is a novel approach to modeling the iterative nature of thermal film growth with realistic lubricant additive molecules.

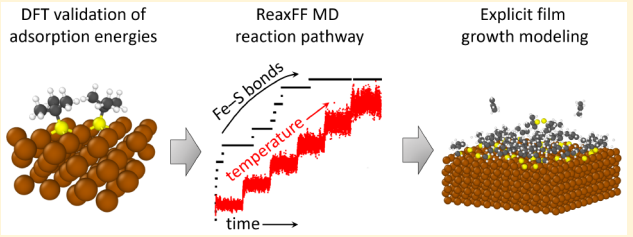

INTRODUCTION

Iron sulfide films are used in a variety of applications including solar energy, water treatment, corrosion, and tribology.[1] In the field of tribology, sulfur-containing molecules are additives in lubricant formulations, where they react, typically with steel, during operation to form protective films.[2] However, the mechanisms by which these important films form are poorly understood because they arise within a sliding contact that cannot be directly probed experimentally. It has been proposed that such films form when the additive molecules thermally decompose as the temperature increases (on the order of ∼1000 K) in sliding interfaces.[3] More recent studies confirmed that shear is necessary to drive the formation of protective films in some sulfur-containing additives[4] and that reaction kinetics are different for thermal vs shear-driven films.[5] In practice, it is likely that both thermal and shear effects contribute to film formation in sliding interfaces. Here, we explore the reactions leading to the formation of a thermal film, with the overall goal of both understanding the thermal film growth on its own, as well as using this information later to contrast the thermal reaction pathway with that driven by shear. We specifically focus on sulfidic films grown on iron, where iron is used as opposed to the more application-relevant steel because the composition and surface structure of iron are better defined.

Early work that studied films from sulfur and iron used macroscale tools to measure friction and wear of organic disufides in oil and then analyzed the composition of the resulting films with post-test characterization such as X-ray photoelectron spectroscopy. Such studies revealed that the friction and/or wear reduction as well as film composition were dependent on the sliding conditions, specifically pressure and temperature, and on the chemical structure of the sulfur compounds.[6−10] More recent studies applied additional surface characterization techniques, such as X-ray absorption near edge structure and atomic force microscopy, and revealed differences between the compositions of films formed during sliding and those of thermo-oxidative films.[11−13] The challenge with extracting information about reaction pathways from the above studies is the complexity of the system, which contains not only the sulfur compound and iron but also base oil and sometimes other additives. As an alternative, it has been shown that the liquid phase lubrication in boundary conditions can be simulated by gaseous species having the same chemical functions as the lubricant additive, which provides a means of isolating the reactions of interest.[14] This approach was implemented in experiments with only sulfide molecules (i.e., no oil) on iron foils in vacuum or ultrahigh vacuum where film growth rates were obtained using a microbalance, and the composition of the film was characterized using various

Received: September 17, 2018
Revised: November 16, 2018
Published: November 26, 2018

DOI: 10.1021/acs.langmuir.8b03170
Langmuir 2018, 34, 15681−15688

techniques. Such studies explored the reaction rates and film compositions of dimethyl disulfide,[3,15] carbon disulfide,[16] and diethyl disulfide[1,3] on iron. These studies showed that the reaction rate varied with temperature and pressure, and analyses suggested that the trends could be explained by a two-stage film formation process where the reaction initially slows due to the formation of a saturated sulfur layer but then resumes at higher temperatures as sulfur diffuses into the substrate.

Experimental studies have been complemented by molecular dynamics (MD) simulations, mostly focused on self-assembled monolayers. Previous simulation work dealing with alkanethiols has been primarily carried out on ideal gold or copper surfaces.[17−20] There are, however, select simulation studies with sulfur-containing molecules and iron surfaces, both investigating corrosion inhibitors on Fe(110). Specifically, simulations were used to explore the adsorption behavior of three thiazole derivatives in sulfuric acid solution[21] and the packing of a self-assembled 2-mercapto-5-methyl-1,3,4-thiadiazole film.[22] Both of these studies used classical MD with the nonreactive COMPASS force field.[23]

Although classical MD can provide insight into the behavior of sulfur-based films, connectivity between atoms is predefined in such simulations, so they cannot capture the formation of films through covalent bonding with a surface. The most accurate way to model the formation and breaking of covalent bonds is by the use of first-principles quantum calculations. However, this approach is often too computationally intensive to model the full dynamic evolution of a system. The alternative is a reactive potential, which uses a bond order to implicitly describe chemical bonding.[24] Reactive potentials have been used to model hydrocarbon film growth via deposition of ethylene and acetylene on diamond[25−27] and acetylene on Ag(111).[28] One of the most commonly used reactive potentials, and the one used in this study because of the availability of parameters for the atoms in our system, is ReaxFF.[29]

ReaxFF parameters have been developed to model the reaction of thiol molecules with surfaces including gold[30−32] and copper.[33] ReaxFF has also been used to model Fischer−Tropsch synthesis, with parameters developed to describe the interactions of iron or iron carbide surfaces with hydrogen and carbon monoxide.[34−36] One ReaxFF parameter set has also been developed that includes both sulfur and iron,[37] albeit not specifically for reactions between organic sulfur compounds and iron. Although the parameters were originally developed to model pyrite (FeS_2), here, we demonstrate that it can also capture the adsorption of di-*tert*-butyl disulfide molecules and radicals derived from them on iron surfaces.

As summarized above, experimental techniques have been used to investigate the reaction rates and compositions of films grown on iron with simple sulfur-containing molecules in the gas phase. However, such experiments are limited to model molecules, i.e., not actual additives, and do not directly provide information about reaction pathways at the atomic scale. Simulations are ideally suited to address this limitation, but, typically, they are based on an assumed surface film morphology and coverage. This assumption has been made because standard, nonreactive interaction potentials are unable to reproduce the chemical processes of film formation, while the time necessary to treat the entire film formation using the much more time-consuming reactive potentials may exceed the available computational capabilities. While reactive simulations have begun to be utilized to model film growth, none yet have been applied to study the interactions of sulfur-containing molecules on iron.

In this work, to address the gap identified above, we explore the thermal film formation process of di-*tert*-butyl disulfide on iron by using reactive MD. Di-*tert*-butyl disulfide is an extreme pressure additive that is commonly used in applied interfacial systems and is well-studied experimentally.[38] The applicability of the reactive potential for this model system is justified by the comparison of adsorption energies and distances to ab initio calculations. Then, reactive MD simulations of di-*tert*-butyl disulfide on an Fe(100) surface are run at temperatures representative of flash temperatures expected in sliding contacts.[3] We initially analyze the dynamics of individual di-*tert*-butyl disulfide molecules on the iron surface to characterize the reaction pathway, including decomposition and chemisorption of the molecule. The rate limiting step in this process is then identified from simulations where the temperature is ramped up in a stepwise manner. Next, the initial stages of film growth are explicitly modeled. While we omit a base oil solvent for the sake of simplicity, we mimic the iterative nature of such film formation by introducing the molecules in several "waves" so that each group of molecules has sufficient time to undergo the necessary reactions to chemisorb to the surface. This approach represents the next step toward modeling dynamic thermal film growth with real, application-relevant molecules by the use of a reactive potential. It is applied here to describe the film formed by the interaction of di-*tert*-butyl disulfide with iron but can be applied subsequently to explore the growth of other films on a variety of surfaces.

EXPERIMENTAL SECTION

Density Functional Theory. Spin-polarized density functional theory (DFT) calculations were performed by using the Vienna Ab-Initio Simulation Package (VASP).[39−44] To describe the interaction between the core and the valence electrons, the projector augmented wave (PAW)[45] method was applied. van der Waals (vdW) interactions were considered in the calculations via the optimized Becke86[46] van der Waals (optB86b-vdW)[47,48] exchange−correlation functional.

The calculation parameters were converged with respect to the total energy within 1 meV. For relaxations, a tight convergence criterion of 10^{-5} eV on the total energy in the self-consistency cycle was used, while for static calculations, a value of 10^{-6} eV was applied. In both cases, a cutoff energy of 600 eV was selected for the plane-wave basis set. The *k*-space integrations were performed using a 2 × 2 × 1 Monkhorst−Pack mesh,[49,50] static calculations employed the tetrahedron method with Blöchl corrections, and relaxations featured Gaussian smearing with a width of 0.05 eV. A conjugate gradient algorithm was used to carry out the relaxations during which the atomic nuclei were displaced while keeping the shape and volume of the cell constant until all forces were smaller than 0.1 eV/nm.

To model adsorption under the DFT framework, a supercell was constructed consisting of an iron surface and either a di-*tert*-butyl disulfide molecule or a *tert*-butyl thiyl radical derived from it. The geometry of the molecule was optimized by performing a relaxation of the isolated molecule in a cubic box of 1.2 nm side length, keeping the relaxation parameters consistent with the rest of the calculations. For the iron surface, two adsorption surfaces, Fe(110) and Fe(100), were considered in this study. To model these surfaces, orthogonal (4 × 6) and (4 × 4) surface slabs of four atomic layers of bcc Fe were constructed by using a lattice constant of 0.287 nm. The resulting slab surface areas of 1.148 × 1.218 nm and 1.148 × 1.118 nm reduced the effect of the interaction between the adsorbed molecule and its mirror image on the total energy to less than 1 meV/atom. To avoid slab−

DOI: 10.1021/acs.langmuir.8b03170
Langmuir 2018, 34, 15681−15688

slab interactions, a vacuum space of 2.1 nm was introduced to the supercell. Dipole corrections were applied to compensate for the artificial electrostatic potential introduced by the periodic boundary conditions in the supercell approximation. The resulting slabs were relaxed to obtain the initial surface geometries used in the adsorption calculations. During these relaxations, the atoms of the lowest layer were kept fixed at the bulk-like positions, while the rest of the atoms were allowed to move in all directions. The di-*tert*-butyl disulfide molecule or the *tert*-butyl thiyl radical was placed on top of the surface, followed by a relaxation. For each relaxed system, a static calculation with higher accuracy was carried out to determine the total energy. The relaxed structures on the (100) surface are shown in Figure 1.

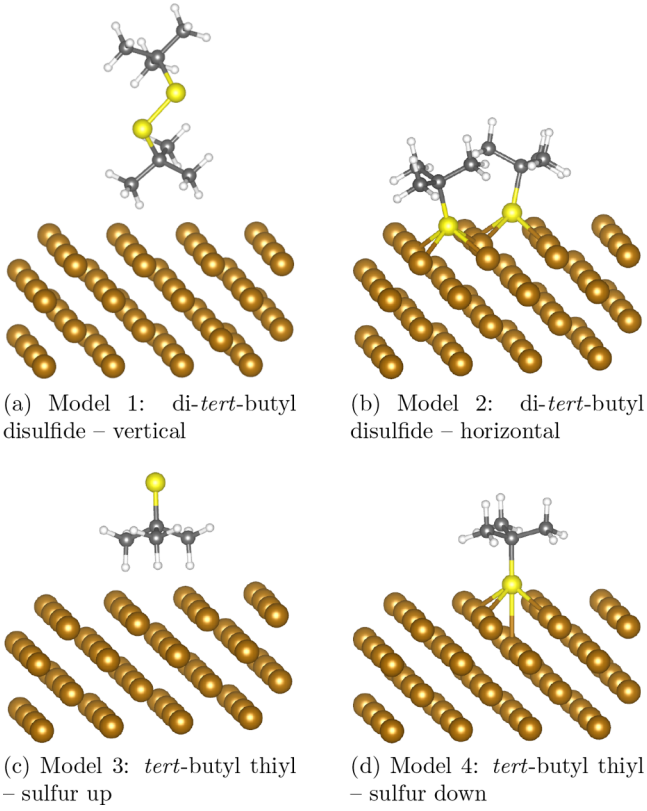

(a) Model 1: di-*tert*-butyl disulfide – vertical

(b) Model 2: di-*tert*-butyl disulfide – horizontal

(c) Model 3: *tert*-butyl thiyl – sulfur up

(d) Model 4: *tert*-butyl thiyl – sulfur down

Figure 1. Equilibrium geometries from DFT for the four adsorption configurations on an Fe(100) surface. Atoms of Fe are brown, S are yellow, C are gray, and H are white.

Molecular Dynamics Simulations. The MD model consisted of di-*tert*-butyl disulfide molecules interacting with bcc iron. Initial atomic configurations were created in Virtual Nano Lab (VNL),[51] with di-*tert*-butyl disulfide atom coordinates downloaded from Pubchem.[52] Minimization and dynamics simulations were performed with the LAMMPS[53] simulation package. All atomic interactions were modeled by using ReaxFF[29] with a parameter set from Shin et al.[37] Visual analysis of the simulations was done using the OVITO[54] visualization package.

The lateral boundaries of the simulation box were periodic, while in the direction normal to the surface they were kept fixed at a height that varied depending on the position of the atoms in the system. In dynamics simulations, the time step was 0.25 fs. During these simulations, the three bottom layers of iron atoms were fixed in space, the two central layers of iron were temperature controlled using a Langevin thermostat with a damping factor of 0.025 ps, and Newtonian dynamics were applied to the top three layers of iron as well as the di-*tert*-butyl disulfide molecules. Because of the system size and the small expected temperature gradients, it was not deemed necessary to implement an electron−phonon coupling scheme to better reproduce the thermal conductivity of iron.[55]

Three types of reactive simulations were performed to (i) calculate the adsorption energy and compare it to DFT results, (ii) characterize the reaction pathway and identify the rate limiting step in that reaction, and (iii) model the growth of a thermal film by cyclic addition of di-*tert*-butyl disulfide molecules.

Adsorption Energy Calculation. To ensure that the ReaxFF parameter set used here is applicable to the system being modeled, we first compared adsorption energies and distances to those calculated from DFT. The atom positions from the model systems in the DFT calculations (Figure 1) were imported into LAMMPS. This included di-*tert*-butyl disulfide in two different orientations and the *tert*-butyl thiyl radical in two different orientations, on both the (100) and (110) surfaces of iron. In both cases, the model dimensions were the same as those in the DFT calculations. As discussed later, only the (100) surface was used in subsequent dynamics simulations but both were evaluated here to better test the potential. Systems containing (a) only the molecule/radical, (b) only the iron slab, and (c) the molecule/radical on the iron slab were constructed. Each system was minimized with ReaxFF by using the conjugate gradient algorithm.

Reaction Pathway Characterization. For the reaction pathway simulations, 18 di-*tert*-butyl disulfide molecules with random orientations were placed approximately 0.5 nm above the Fe(100) slab. The slab consisted of 1152 atoms and was 3.44 × 3.44 × 1.14 nm in the *x*, *y*, and *z* directions, respectively (see upper left inset in Figure 2). The model was energy minimized, then dynamics were run, first at 300 K for 0.2 ns and then ramped up to 900 K over 100 ps. This high temperature was chosen both to accelerate the chemical reactions as well as to be consistent with the temperature range expected for a thermal film that occurs in a sliding interface.[3] The trajectory and bonding state of individual atoms were analyzed to characterize the reaction pathway.[56,57] Then, to isolate the rate limiting step, the simulation was repeated but with the temperature ramped up from 300 to 900 K at 100 K increments, with the system held at each temperature for 150 ps. Throughout these simulations, the bond order of each atom was calculated by the ReaxFF potential and recorded. A Python script was written to count the number of bonds between different atom types, where a bond order of 0.3 or more was considered to be a covalent bond.

Film Growth Protocol. The initial model described above was also used as the starting point of the thermal film growth simulations. One cycle of the process is shown in Figure 2. After the addition of the di-*tert*-butyl disulfide molecules at 0.2 nm above the Fe(100) surface, the simulation was run at 300 K for 275 ps. The temperature was then increased linearly to 900 K over 100 ps and held at the final temperature for 245 ps. During the temperature ramp and the constant high temperature simulation, some molecule fragments detached from the surface. To limit how far the atoms in these fragments could travel, a repulsive wall was placed above the surface.[28] At the end of the high-temperature equilibration, any molecules or radicals not bonded to the surface were removed from the model. This was done to mimic the diffusion of molecules or radicals into a much larger reservoir of lubricant, as would be the case in a real lubricated contact. Then, the system was cooled linearly to 300 K over 100 ps. These steps (1−1 through 1−4 in Figure 2) represent the first cycle of the film growth process. The next cycle began by the addition of a second set of 18 di-*tert*-butyl disulfide molecules at 0.9 nm above the surface, then the process started again at step 2−1. The procedure described above for the second cycle was carried out three times, for a total of four cycles of thermal film growth. While we did not explicitly model base oil solvent for simplicity, the approach described above approximates the iterative nature of film formation in a lubricated interface by introducing the molecules in several "waves", so that each group of molecules has sufficient time to undergo the necessary reactions to chemisorb to the surface.

DOI: 10.1021/acs.langmuir.8b03170
Langmuir 2018, 34, 15681−15688

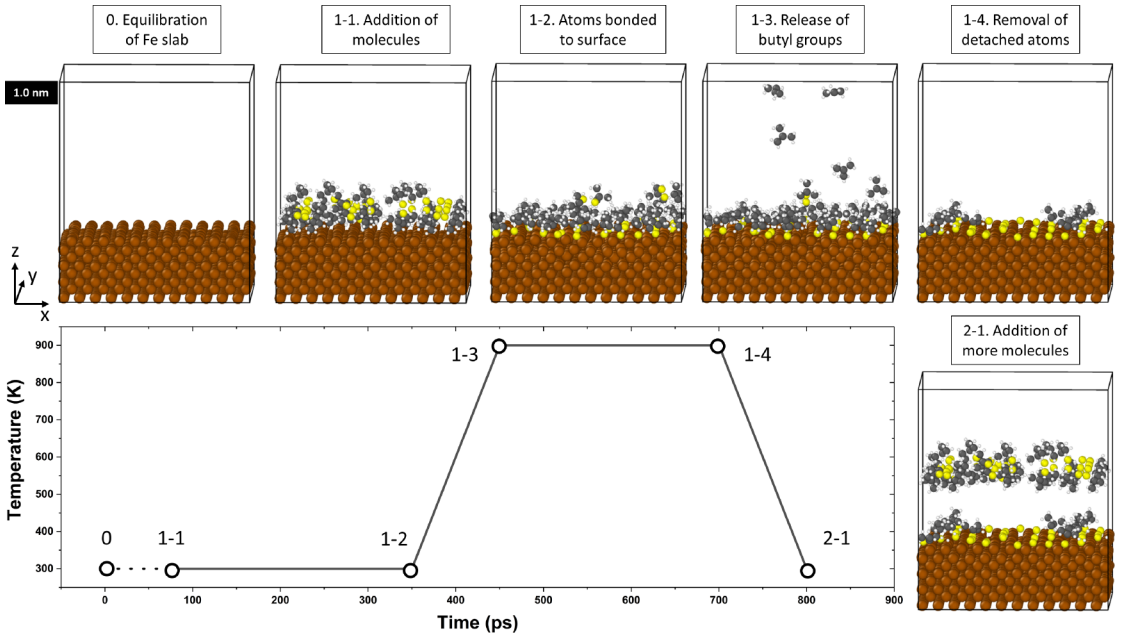

Figure 2. Simulation protocol for iteratively growing a thermal film of di-*tert*-butyl disulfide on an iron surface. The insets show perspective view snapshots of the simulation at points corresponding to the numbers in the plot of temperature vs time, where labels indicate cycle−stage, e.g., 1−2 corresponds to the second stage of the first cycle. Sphere colors are brown for iron, yellow for sulfur, gray for carbon and white for hydrogen.

RESULTS AND DISCUSSION

Validation of the Empirical Model. MD simulations were performed with a ReaxFF parameter set that included both sulfur and iron[37] but was not developed specifically for the model system we are studying here. Therefore, we first confirmed the applicability of this parameter set for model interactions of di-*tert*-butyl disulfide and iron by comparing adsorption energies obtained from the force field to those calculated by using DFT. In both the ReaxFF and DFT calculations, the energies of the molecule/radical, iron slab, and molecule/radical adsorbed on the slab were used to obtain the adsorption energy according to the equation

$$E_{ads} = E_{tot}^{mol+Fe} - (E_{tot}^{mol} + E_{tot}^{Fe}) \quad (1)$$

where E_{tot}^{mol+Fe} is the total energy of the products adsorbed on the Fe slab at the equilibrium distance, E_{tot}^{Fe} is the total energy of the clean Fe slab, and E_{tot}^{mol} is the total energy of the isolated gas-phase disulfide molecule or thiyl radical.

The results are shown in Tables 1 and 2 for the (110) and (100) surfaces, respectively, where the model numbers refer to the configurations shown in Figure 1. The adsorption energies obtained from ReaxFF are comparable to those calculated from DFT in most cases. The agreement is particularly good for the Fe(100) surface for which the difference between DFT and ReaxFF energies is less than 1 eV for all model configurations. The equilibrium distance is defined as the perpendicular distance between the two closest atoms, one belonging to the slab and the other to the molecule or radical. All equilibrium distances are in good agreement, with a maximum difference between DFT and ReaxFF of 0.02 nm. On the basis of the above analysis, we used the (100) surface for all subsequent MD simulations.

Table 1. Comparison of Equilibrium Distances and Adsorption Geometries Calculated with DFT and ReaxFF for the Systems with an Fe(110) Surface

	equilibrium distance (nm)		adsorption energy (eV)	
system	DFT	ReaxFF	DFT	ReaxFF
model 1	0.22	0.20	−0.40	−0.80
model 2	0.15	0.17	−5.21	−3.93
model 3	0.20	0.18	0.11	−0.66
model 4	0.15	0.16	−4.34	−3.26

Table 2. Comparison of Equilibrium Distances and Adsorption Geometries Calculated with DFT and ReaxFF for the Systems with an Fe(100) Surface

	equilibrium distance (nm)		adsorption energy (eV)	
system	DFT	ReaxFF	DFT	ReaxFF
model 1	0.19	0.18	−0.39	−0.94
model 2	0.13	0.11	−5.75	−6.60
model 3	0.18	0.18	−0.72	−0.56
model 4	0.12	0.10	−4.48	−4.23

Reaction Pathway for Iron Sulfide Formation. ReaxFF simulations were initially run at 300 K for 0.2 ns and then ramped up to 900 K to accelerate the chemical reactions. The movement and bonding of individual molecules was tracked to analyze the reaction pathway. A representative case is shown in Figure 3. We observe that the sulfur−sulfur (S−S) bond breaks soon after the molecule approaches the surface. Note that this bond does not break if the molecule is far from the surface, indicating that interactions with the iron caused a weakening of the S−S bond. This is followed by the formation of covalent bonds between sulfur and iron. Finally, the sulfur−carbon (S−C) bond breaks, and a *tert*-butyl group is released. This reaction pathway was observed for multiple initial orientations of the di-*tert*-butyl disulfide relative to the surface. Further, a second set of simulations was run with a time step of 0.1 fs, and the same reaction pathway was observed. This general reaction path—in which the S−S bond breaks, the sulfur atoms bond with the iron surface, and two *tert*-butyl radicals are released—

DOI: 10.1021/acs.langmuir.8b03170
Langmuir 2018, 34, 15681−15688

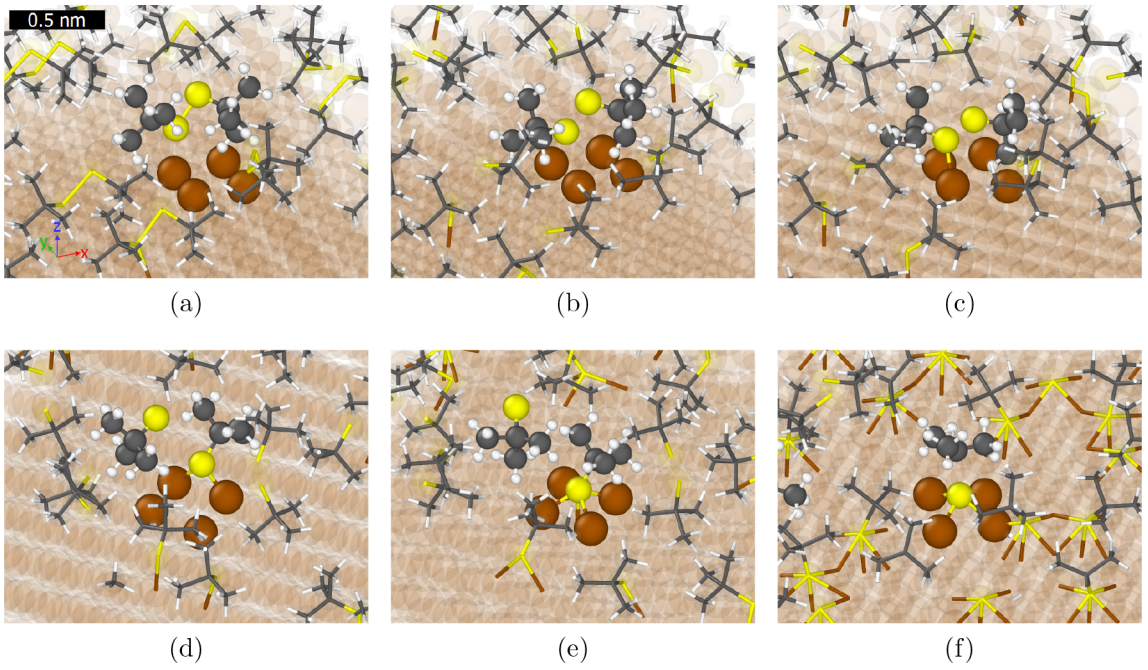

Figure 3. Snapshots from the simulation illustrating the reaction pathway for a representative di-*tert*-butyl disulfide. To highlight the atoms of interest, iron atoms are shown as partially transparent and all other atoms not involved in the reaction are shown in stick representation. Images (a) through (e) correspond to the 300 K stage of the simulation, and (f) was taken from the simulation after the temperature increase to 900 K. The snapshots illustrate the reaction pathway consisting of (a) a di-*tert*-butyl disulfide molecule approaching the surface, (b) breaking of the sulfur−sulfur bond, (c)−(e) formation of sulfur−iron bonds, and (f) breaking of the carbon−sulfur bond and release of a *tert*-butyl group, where only one of the two sulfur atoms that chemisorbed from this di-*tert*-butyl disulfide molecule is highlighted. The stick/sphere colors are the same as in Figure 2.

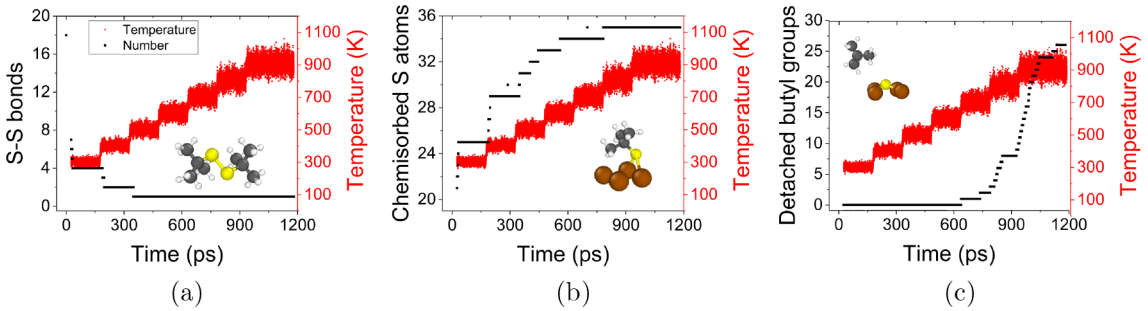

Figure 4. Temperature dependence of the three key steps in the reaction: (a) breaking of the S−S bond in the di-*tert*-butyl disulfide, quantified by the number of S−S bonds; (b) chemical bonding with the surface, quantified by the number of S atoms bonded to the surface; and (c) release of *tert*-butyl groups, quantified by the number of detached *tert*-butyl groups in the simulation.

is consistent with what has been previously proposed for dimethyl and diethyl disulfide on iron based on experimental measurements.[3]

Three key steps can be identified in the reaction described above: breaking of the S−S bond, formation of the iron−sulfur (Fe−S) bond, and release of a *tert*-butyl group via breaking of the S−C bond. Previous work has shown that the S−S bond in disulfides is weak (bond dissociation energies of ∼65 kcal/mol for dialkyldisulfides and ∼50 kcal/mol for diaryldisulfides) compared to the S−C bond (∼73 kcal/mol in dimethylsulfide and ∼77 kcal/mol in diethylsulfide).[58] This indicates that the S−S bond should break at lower temperatures than the S−C bond, so the release of the *tert*-butyl group is likely to be the rate limiting step in the reaction.

To confirm that our simulation reproduces this expectation, we performed simulations in which the temperature was ramped up from 300 to 900 K at 100 K increments, as illustrated in Figure 4. Figure 4a shows that the S−S bonds start breaking at room temperature and are broken in all di-*tert*-butyl disulfide molecules before the temperature reaches 500 K. The formation of Fe−S bonds occurs somewhat more slowly (Figure 4b), with almost all of the S atoms in the system bonded with the Fe by the time the temperature reaches 800 K. However, the slowest reaction is clearly the breaking of the S−C bond, which, as shown in Figure 4c, does not start happening until the temperature reaches 700 K, and only ∼20% of the *tert*-butyl groups have been released by the end of the temperature plateau at 800 K. Increasing the temperature to 900 K finally pushes the fraction of detached *tert*-butyl groups beyond 70%. The observation from our simulations that organic moieties are not easily released from the surface is consistent with the presence of carbon in experimental thermal films.[3] In general, a comparison of the temperatures at which each reaction occurs indicates that, as expected, the release of

DOI: 10.1021/acs.langmuir.8b03170
Langmuir 2018, 34, 15681−15688

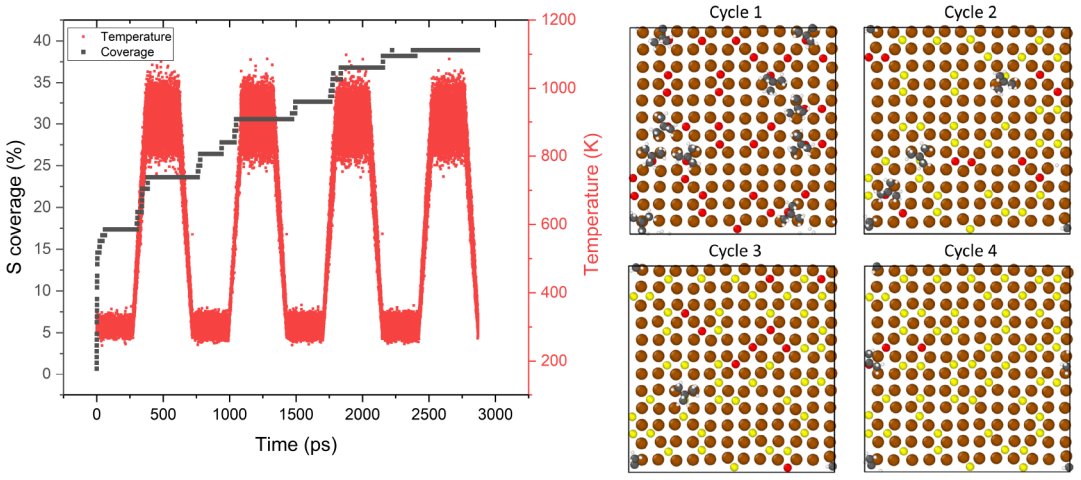

Figure 5. (a) Sulfur coverage on the iron surface and model temperature during four cycles of the film growth protocol. (b) Top view snapshots of the model after each of the four cycles. Only the topmost Fe atoms and S atoms or *tert*-butyl thiyl radicals bonded to the surface are shown. S atoms that bonded to the surface during a given cycle are shown in red while those that bonded to the surface in a previous cycle are shown in yellow.

the *tert*-butyl group through breaking of the S−C bond is the rate liming step in the reaction of di-*tert*-butyl disulfide with an iron surface.

Modeling Thermal Film Growth. The film growth protocol illustrated in Figure 2 was run four times. Throughout the simulation, the sulfur coverage was calculated from the number of sulfur atoms covalently bonded to the iron surface divided by the total number of available bonding sites (in this case 144). The coverage and actual temperature are shown in Figure 5 along with top view snapshots of the surface and atoms bonded to the surface at the end of each cycle. During the 300 K stage of the first cycle, we observe that the sulfur coverage increases rapidly, up to 18%. There are a few additional bonds formed during the temperature ramp, and then the coverage remains constant during most of the 900 K stage of the first cycle. During this time, S−C bonds break, enabling *tert*-butyl groups to leave the surface; these radicals are subsequently removed from the simulation. The reaction pathway is the same as that described above based on analysis of individual molecules. Further, we observe that, in most cases, S atoms from a given di-*tert*-butyl disulfide molecule bond with Fe at adjacent sites on the surface. At the end of the first cycle, the sulfur coverage is at 24%.

The second and third cycles exhibit similar behavior as the first, with sulfur chemisorption occurring during the 300 K phase and then *tert*-butyl removal occurring during the 900 K phase. However, the rate of increase in coverage with time is slower each cycle due to the decreasing availability of reaction sites. An analysis of Figure 5b suggests that film growth after the first cycle occurs by new sulfur atoms preferentially adsorbing to those iron atoms that are least saturated by previously adsorbed sulfur atoms. At the end of the second and third cycles of tribofilm growth, the surface coverage is 31% and 37%, respectively. During the fourth cycle, few additional reactions occurred and the film reached a maximum coverage of 39%. This is likely near the maximum coverage that can be achieved within the nanosecond-scale duration of a reactive MD simulation. Unfortunately, the results cannot be compared directly to experimental observations of Fe−S film growth over minutes of reaction time.[1,3,15,16] However, the simulations complement experimental approaches since the simulations enable direct observation of individual species involved in reactions with surfaces and their behavior under various conditions, providing information about the initial stages of film formation that is not currently accessible by the use of even highly resolving surface analytical methods.

To evaluate the friction reducing potential of a fully grown Fe−S film, we performed some preliminary simulations of moving a hemispherical Fe(111) tip with a diameter of 1.38 nm over the surface at normal loads ranging from 0.7 to 5.5 nN, equivalent to 0.5 to 3.7 GPa. This was done on a clean Fe(100) surface and on a surface covered with 144 S atoms, which translates into 100% coverage. We analyzed the friction-vs-load behavior, $F(L) = \mu L + F_0$, where F is the friction force, μ is the coefficient of friction, L is the normal load, and F_0 is the load-independent friction at zero load that is generally related to adhesion.[59] The friction coefficient μ was reduced by 50% in the system with the Fe−S film, and the dominating load-independent force F_0 was reduced by more than 85% of the value obtained with the clean Fe(100) surface. This led to an overall reduction of friction force by a factor of approximately six. The results of this preliminary simulation are consistent with experimental observations of the benefits of sulfur on iron surfaces, including more sulfur content leading to lower wear[7] and higher seizure load.[3]

SUMMARY AND CONCLUSIONS

Films formed by chemical reactions between ferrous surfaces and di-*tert*-butyl disulfide—an important extreme pressure additive, e.g., used in gears—are critical to the efficiency and useful lifetime of mechanical components with lubricated interfaces. Here, we modeled the initial steps of the thermal formation of such a protective film using molecular dynamics simulations with a reactive empirical potential, validated for the most relevant interactions by the comparison of adsorption energies to DFT calculations. The empirical model was used to identify the reaction pathway leading to iron sulfide: the S−S bond in the di-*tert*-butyl disulfide breaks, the S atoms bond to the Fe(100) surface, and then *tert*-butyl groups are released. This observation is consistent with pathways for reactions between sulfur-containing molecules and iron previously

DOI: 10.1021/acs.langmuir.8b03170
Langmuir 2018, 34, 15681−15688

proposed based on experimental measurements. Next, simulations performed at increased temperatures suggested that the breaking of S−C bonds that enabled *tert*-butyl radical release was the rate limiting step of the reaction. With this understanding of the steps associated with surface reactions, we implemented a simulation protocol to mimic the process by which films form in lubricated interfaces where the surfaces are repeatedly exposed to temperature increases due to sliding. Using this approach, the onset of the formation of an iron sulfide film was captured.

Future research efforts specifically focused on di-*tert*-butyl disulfide and ferrous surfaces can build on the foundations established in this work. For example, here we mimicked the replenishment of the molecules at the surface through lubricant flow by manually adding new molecules to the system. However, more complex models can explicitly incorporate base oil molecules and liquid flow to confirm that the reactions we observe here are indeed representative of the precursors of a thermal film in a lubricated interface. Further, in practice, these films are formed through the combined effects of frictional heating and mechanical stress. Future models can incorporate load and/or shear by introducing an iron counterbody that confines the additive molecules, as demonstrated by the preliminary simulations of frictional sliding described in the previous section. Such an approach can be used to differentiate the effect of temperature from that of shear in driving chemical reactions. Moreover, the thermal film growth simulation approach was demonstrated here with an ideal Fe(100) surface. This choice reflects the assumption that nascent iron surfaces are exposed as surfaces slide relative to one another but is a simplified approximation of the likely surface composition and structure. The approach demonstrated here can be extended to study the interaction of di-*tert*-butyl disulfide (or other additives) with other iron surfaces or with iron oxide. Lastly, thermal films, both with sulfur-containing molecules and otherwise, are present and important in many different applications. Therefore, the approach demonstrated here can be applied to explore the initial stages of film formation in a variety of scientific and engineering fields.

AUTHOR INFORMATION

Corresponding Author

*E-mail: amartini@ucmerced.edu. Phone: +1 (209) 228-2354.

ORCID

Ashlie Martini: 0000-0003-2017-6081

Notes

The authors declare no competing financial interest.

ACKNOWLEDGMENTS

This work was supported by the National Science Foundation through grant number CMMI-1634354 and the Austrian COMET-Program (Project K2, XTribology, no. 849109). Part of this work was carried out at the "Excellence Centre of Tribology" (AC2T research GmbH).

REFERENCES

(1) Ocampo-Macias, T.; Lara-Romero, J.; Huirache-Acuña, R.; Alvarado-Flores, J. J.; López-Tinoco, J.; Chiñas-Castillo, F.; Jimenez-Sandoval, S.; Paraguay-Delgado, F.; Reyes-Rojas, A. Synthesis of iron sulfide films through solid-gas reaction of iron with diethyl disulfide. *J. Sulfur Chem.* **2015**, *36*, 385−394.

(2) Rudnick, L. R. *Lubricant Additives: Chemistry and Applications*, 3rd ed.; CRC Press: Boca Raton, FL, 2017.

(3) Kaltchev, M.; Kotvis, P. V.; Blunt, T. J.; Lara, J.; Tysoe, W. T. A molecular beam study of the tribological chemistry of dialkyl disulfides. *Tribol. Lett.* **2001**, *10*, 45−50.

(4) Zhang, J.; Spikes, H. On the Mechanism of ZDDP Antiwear Film Formation. *Tribol. Lett.* **2016**, *63*, 24.

(5) Dorgham, A.; Neville, A.; Ignatyev, K.; Mosselmans, F.; Morina, A. An in situ synchrotron XAS methodology for surface analysis under high temperature, pressure, and shear. *Rev. Sci. Instrum.* **2017**, *88*, 015101.

(6) Bird, R. J.; Galvin, G. D. The application of photoelectron spectroscopy to the study of E.P. films on lubricated surfaces. *Wear* **1976**, *37*, 143−167.

(7) Baldwin, B. A. Relationship between Surface Composition and Wear: an X-ray Photoelectron Spectroscopic Study of Surfaces Tested with Organosulfur Compounds. *ASLE Trans.* **1976**, *19*, 335−344.

(8) Wheeler, D. R. X-ray photoelectron spectroscopic study of surface chemistry of dibenzyl disulfide on steel under mild and severe wear conditions. *Wear* **1978**, *47*, 243−254.

(9) Plaza, S. Some Chemical Reactions of Organic Disulfides in Boundary Lubrication. *ASLE Trans.* **1986**, *30*, 493−500.

(10) Zhang, J.; Yang, S.; Liu, W.; Xue, Q. A study of 2-(n-alkyldithio)-benzoxazoles as novel additives. *Tribol. Lett.* **1999**, *7*, 173−177.

(11) Najman, M.; Kasrai, M.; Bancroft, G. X-ray Absorption Spectroscopy and Atomic Force Microscopy of Films Generated from Organosulfur Extreme-Pressure (EP) Oil Additives. *Tribol. Lett.* **2003**, *14*, 225−235.

(12) Zhang, Z.; Najman, M.; Kasrai, M.; Bancroft, G. M.; Yamaguchi, E. S. Study of interaction of EP and AW additives with dispersants using XANES. *Tribol. Lett.* **2005**, *18*, 43−51.

(13) Costello, M. T.; Kasrai, M. Study of surface films of overbased sulfonates and sulfurized olefins by X-Ray Absorption Near Edge Structure (XANES) spectroscopy. *Tribol. Lett.* **2006**, *24*, 163−169.

(14) Tannous, J.; de Bouchet, B. M. I.; Le-Mogne, T.; Charles, P.; Martin, J. M. Contribution of gas phase lubrication in understanding tribochemistry of organosulphur compounds. *Tribol.-Mater., Surf. Interfaces* **2007**, *1*, 98−104.

(15) Lara, J.; Blunt, T.; Kotvis, P.; Riga, A.; Tysoe, W. T. Surface Chemistry and Extreme-Pressure Lubricant Properties of Dimethyl Disulfide. *J. Phys. Chem. B* **1998**, *102*, 1703−1709.

(16) Lara, J.; Surerus, K. K.; Kotvis, P.; Contreras, M. E.; Rico, J. L.; Tysoe, W. T. The surface and tribological chemistry of carbon disulfide as an extreme-pressure additive. *Wear* **2000**, *239*, 77−82.

(17) Dishner, M. H.; Hemminger, J. C.; Feher, F. J. Direct observation of substrate influence on chemisorption of methanethiol adsorbed from the gas phase onto the reconstructed Au (111) surface. *Langmuir* **1997**, *13*, 2318−2322.

(18) Yamada, R.; Wano, H.; Uosaki, K. Effect of temperature on structure of the self-assembled monolayer of decanethiol on Au (111) surface. *Langmuir* **2000**, *16*, 5523−5525.

(19) Love, J. C.; Estroff, L. A.; Kriebel, J. K.; Nuzzo, R. G.; Whitesides, G. M. Self-assembled monolayers of thiolates on metals as a form of nanotechnology. *Chem. Rev.* **2005**, *105*, 1103−1170.

(20) Adams, H. L.; Garvey, M. T.; Ramasamy, U. S.; Ye, Z.; Martini, A.; Tysoe, W. T. Shear-Induced Mechanochemistry: Pushing Molecules Around. *J. Phys. Chem. C* **2015**, *119*, 7115.

(21) Khaled, K.; Amin, M. A. Corrosion monitoring of mild steel in sulphuric acid solutions in presence of some thiazole derivatives-molecular dynamics, chemical and electrochemical studies. *Corros. Sci.* **2009**, *51*, 1964−1975.

(22) Zhou, J.; Chen, S.; Zhang, L.; Feng, Y.; Zhai, H. Studies of protection of self-assembled films by 2-mercapto-5-methyl-1, 3, 4-thiadiazole on iron surface in 0.1 M H_2SO_4 solutions. *J. Electroanal. Chem.* **2008**, *612*, 257−268.

(23) Sun, H. COMPASS: an ab initio force-field optimized for condensed-phase applications overview with details on alkane and benzene compounds. *J. Phys. Chem. B* **1998**, *102*, 7338−7364.

DOI: 10.1021/acs.langmuir.8b03170
Langmuir 2018, 34, 15681−15688

(24) Senftle, T. P.; Hong, S.; Islam, M. M.; Kylasa, S. B.; Zheng, Y.; Shin, Y. K.; Junkermeier, C.; Engel-Herbert, R.; Janik, M. J.; Aktulga, H. M.; Vertraelen, T.; Grama, A.; van Duin, A. C. T. The ReaxFF reactive force-field: development, applications and future directions. *NPJ. Computational Materials* **2016**, *2*, 15011.
(25) Qi, L.; Sinnott, S. B. Atomistic simulations of organic thin film deposition through hyperthermal cluster impacts. *J. Vac. Sci. Technol., A* **1998**, *16*, 1293.
(26) Qi, L.; Sinnott, S. B. Generation of 3D hydrocarbon thin films via organic molecular cluster collisions. *Surf. Sci.* **1998**, *398*, 195−202.
(27) Hu, Y.; Sinnott, S. B. Molecular dynamics simulation of thin film nucleation through molecular cluster beam deposition: Effect of incident angle. *Nucl. Instrum. Methods Phys. Res., Sect. B* **2002**, *195*, 329−338.
(28) Zarshenas, M.; Czerwinski, B.; Leyssens, T.; Moshkunov, K.; Delcorte, A. D. Molecular Dynamics Simulations of Hydrocarbon Film Growth from Acetylene Monomers and Radicals: Effect of Substrate Temperature. *J. Phys. Chem. C* **2018**, *122*, 15252−15263.
(29) van Duin, A. C. T.; Dasgupta, S.; Lorant, F.; Goddard, W. A. ReaxFF: A Reactive Force Field for Hydrocarbons. *J. Phys. Chem. A* **2001**, *105*, 9396−9409.
(30) Jarvi, T. T.; van Duin, A. C. T.; Nordlund, K.; Goddard, W. A. Development of Interatomic ReaxFF Potentials for Au−S−C−H Systems. *J. Phys. Chem. A* **2011**, *115*, 10315−10322.
(31) Bae, G.-T.; Aikens, C. M. Improved ReaxFF Force Field Parameters for Au−S−C−H Systems. *J. Phys. Chem. A* **2013**, *117*, 10438−10446.
(32) Vasumathi, V.; Fajin, J. L. C.; Cordeiro, M. N. D. S. How reliable is the ReaxFF potential for describing the structure of alkanethiols on gold? A molecular dynamics study. *International Journal of Modeling, Simulation, and Scientific Computing* **2014**, *5*, 1441011.
(33) Yeon, J.; Adams, H. L.; Junkermeier, C. E.; van Duin, W. T.; Adri C. T, Tysoe; Martini, A. Development of a ReaxFF Force Field for Cu/S/C/H and Reactive MD Simulations of Methyl Thiolate Decomposition on Cu (100). *J. Phys. Chem. B* **2018**, *122*, 888.
(34) Zou, C.; van Duin, A. C. T. Investigation of Complex Iron Surface Catalytic Chemistry Using the ReaxFF Reactive Force Field Method. *JOM* **2012**, *64*, 1426−1437.
(35) Zou, C.; van Duin, A. C. T.; Sorescu, D. C. Theoretical Investigation of Hydrogen Adsorption and Dissociation on Iron and Iron Carbide Surfaces Using the ReaxFF Reactive Force Field Method. *Top. Catal.* **2012**, *55*, 391−401.
(36) Islam, M. M.; Zou, C.; van Duin, A. C. T.; Raman, S. Interactions of hydrogen with the iron and iron carbide interfaces: a ReaxFF molecular dynamics study. *Phys. Chem. Chem. Phys.* **2016**, *18*, 761−771.
(37) Shin, Y. K.; Kwak, H.; Vasenkov, A. V.; Sengupta, D.; van Duin, A. C. Development of a ReaxFF Reactive Force Field for Fe/Cr/O/S and Application to Oxidation of Butane over a Pyrite-Covered Cr_2O_3 Catalyst. *ACS Catal.* **2015**, *5*, 7226−7236.
(38) Quinn, T. F. *Physical analysis for tribology*; Cambridge University Press: 2005.
(39) Kresse, G.; Hafner, J. Ab initio molecular dynamics for liquid metals. *Phys. Rev. B: Condens. Matter Mater. Phys.* **1993**, *47*, 558−561.
(40) Kresse, G.; Hafner, J. Norm-conserving and ultrasoft pseudopotentials for first-row and transition elements. *J. Phys.: Condens. Matter* **1994**, *6*, 8245−8257.
(41) Kresse, G.; Hafner, J. Ab initio molecular-dynamics simulation of the liquid-metal-amorphous-semiconductor transition in germanium. *Phys. Rev. B: Condens. Matter Mater. Phys.* **1994**, *49*, 14251−14269.
(42) Kresse, G.; Furthmüller, J. Efficient iterative schemes for ab initio total-energy calculations using a plane-wave basis set. *Phys. Rev. B: Condens. Matter Mater. Phys.* **1996**, *54*, 11169.
(43) Kresse, G.; Furthmüller, J. Efficiency of ab-initio total energy calculations for metals and semiconductors using a plane-wave basis set. *Comput. Mater. Sci.* **1996**, *6*, 15−50.
(44) Kresse, G.; Joubert, D. From ultrasoft pseudopotentials to the projector augmented-wave method. *Phys. Rev. B: Condens. Matter Mater. Phys.* **1999**, *59*, 1758−1775.
(45) Blöchl, P. E. Projector augmented-wave method. *Phys. Rev. B: Condens. Matter Mater. Phys.* **1994**, *50*, 17953−17979.
(46) Becke, A. D. On the large-gradient behavior of the density functional exchange energy. *J. Chem. Phys.* **1986**, *85*, 7184−7187.
(47) Klimeš, J.; Bowler, D. R.; Michaelides, A. Chemical accuracy for the van der Waals density functional. *J. Phys.: Condens. Matter* **2010**, *22*, 022201.
(48) Klimeš, J.; Bowler, D. R.; Michaelides, A. Van der Waals density functionals applied to solids. *Phys. Rev. B: Condens. Matter Mater. Phys.* **2011**, *83*, 195131.
(49) Monkhorst, H. J.; Pack, J. D. Special points for Brillouin-zone integrations. *Phys. Rev. B* **1976**, *13*, 5188−5192.
(50) Methfessel, M.; Paxton, A. T. High-precision sampling for Brillouin-zone integration in metals. *Phys. Rev. B: Condens. Matter Mater. Phys.* **1989**, *40*, 3616−3621.
(51) Virtual NanoLab 2017.0, Synopsys QuantumWise A/S. www.quantumwise.com.
(52) Kim, S.; Thiessen, P. A.; Bolton, E. E.; Chen, J.; Fu, G.; Gindulyte, A.; Han, L.; He, J.; He, S.; Shoemaker, B. A.; Wang, J.; Yu, B.; Zhang, J.; Bryant, S. H. PubChem Substance and Compound databases. *Nucleic Acids Res.* **2016**, *44*, D1202−D1213.
(53) Plimpton, S. Fast Parallel Algorithms for Short-Range Molecular Dynamics. *J. Comput. Phys.* **1995**, *117*, 1−19.
(54) Stukowski, A. Visualization and analysis of atomistic simulation data with OVITO-the Open Visualization Tool. *Modell. Simul. Mater. Sci. Eng.* **2010**, *18*, 015012.
(55) Eder, S. J.; Cihak-Bayr, U.; Bianchi, D.; Feldbauer, G.; Betz, G. Thermostat Influence on the Structural Development and Material Removal during Abrasion of Nanocrystalline Ferrite. *ACS Appl. Mater. Interfaces* **2017**, *9*, 13713−13725.
(56) Yeon, J.; He, X.; Martini, A.; Kim, S. Mechanochemistry at Solid Surfaces: Polymerization of Adsorbed Molecules by Mechanical Shear at Tribological Interfaces. *ACS Appl. Mater. Interfaces* **2017**, *9*, 3142−3148.
(57) Khajeh, A.; He, X.; Yeon, J.; Kim, S.; Martini, A. Mechanochemical Association Reaction of Interfacial Molecules Driven by Shear. *Langmuir* **2018**, *34*, 5971−5977.
(58) Dénès, F.; Pichowicz, M.; Povie, G.; Renaud, P. Thiyl Radicals in Organic Synthesis. *Chem. Rev.* **2014**, *114*, 2587−2693.
(59) Eder, S. J.; Vernes, A.; Betz, G. On the Derjaguin offset in boundary-lubricated nanotribological systems. *Langmuir* **2013**, *29*, 13760−13772.

DOI: 10.1021/acs.langmuir.8b03170
Langmuir 2018, 34, 15681−15688